Supplementary Material for: Deformable Vesicles Interacting in a Nematic Liquid Crystal

F.E. Mackay,[*a] **and C. Denniston,**[a]

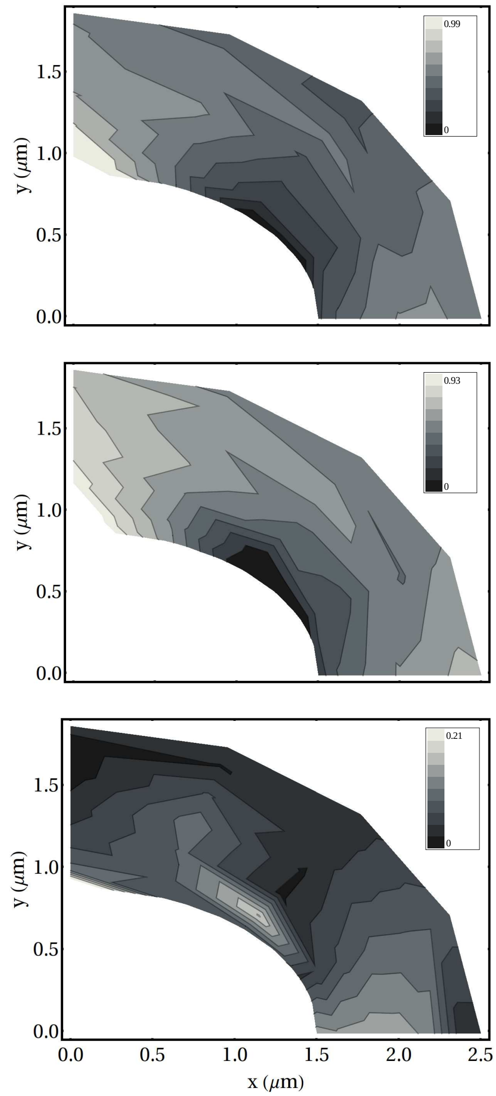

Fig. S1 Interaction energy between a pair of deformable vesicles, with spring constants $k_1 = 0.2$ and $k_2 = 4.0$, in the xy-plane. One vesicle is fixed at $(0, 0)$, and the system energy (in $fg \cdot \mu m^2/\mu s^2$ relative to the minimum attained value) is measured for various positions of the second particle. The solid white areas correspond to regions that were not measured. The plots correspond to: the total (liquid crystal plus spring) energy (top panel), the liquid crystal free energy (middle panel), and the spring energy (lower panel).

Figure S1 is an expanded version of Figure 5 in the main manuscript, showing not only the total interaction energy (top panel), but also the individual components, consisting of the liquid crystal free energy

[a] *Department of Applied Mathematics, The University of Western Ontario, London, Ontario N6A 5B8, Canada; E-mail: fmackay@uwo.ca*

(middle panel), and the spring energy (lower panel). Note the correspondence between regions where the liquid crystal energy is minimized, and maxima in the spring energy. In addition a Mathematica notebook (3D_EnergyPlots.nb) has been provided, which presents 3D versions of the interaction energies given in the above Figure S1.

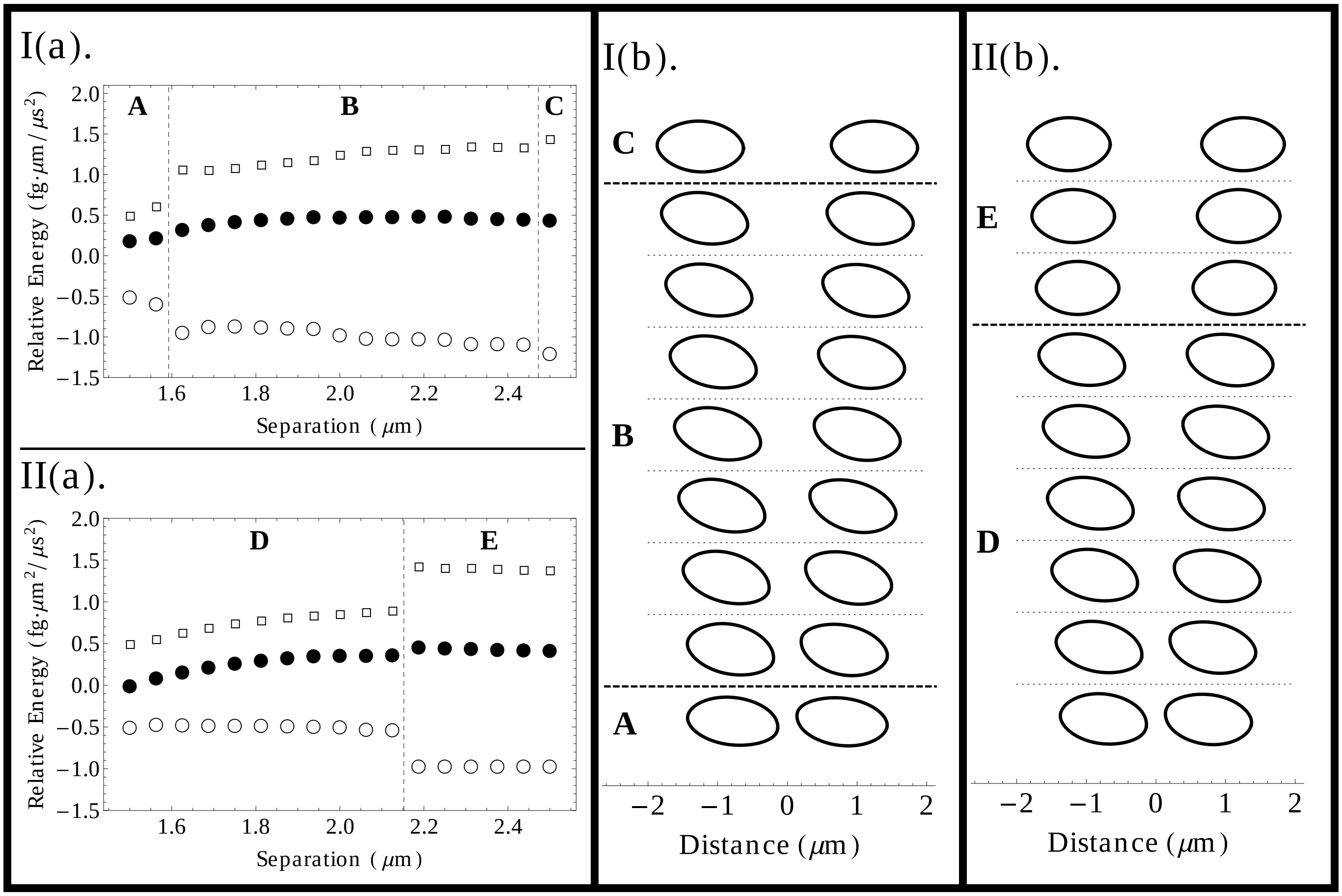

Fig. S2 Additional example of the interaction between deformable particles separated along the x-axis, with the bulk liquid crystal director orientation along the y-axis. Plots I(a), and II(a) show the relative changes in the free energy as a function of particle separation, with the associated particle shapes given in plots I(b), and II(b). Hollow circles represent the elastic energy of the springs, which has been shifted so that the closest particle separation corresponds to a value of $-0.5\ fg \cdot \mu m^2/\mu s^2$, hollow squares correspond to the liquid crystal free energy, shifted to $0.5\ fg \cdot \mu m^2/\mu s^2$ for the closest separation, and the total system energy, which is set to $0.0\ fg \cdot \mu m^2/\mu s^2$ at closest separation, is denoted by filled circles. Plots I: spring constants: $k_1 = 0.1,\ k_2 = 2.0$. Plots II: $k_1 = 0.2,\ k_2 = 2.0$.

Figure S2 is similar to Figure 7 in the main manuscript, providing further examples of the interaction energies and particle shapes for particles separated along the x-axis. As can be seen, the behavior is quite similar to that shown in Figure 7; for large separations, the shapes are the same as for an isolated particle, and the change to these symmetric shapes occurs at a larger separation for the particles in Figure S2 I. In addition, a further shape change, from Region A to B is also observed in Figure S2 I. The locations of the various shape changes, and whether or not a change occurs results from a direct competition between the spring and liquid crystal energies. (See the main manuscript for further detail).

Figure S3 provides detailed results for the interaction of particles separated along the y-axis, which corresponds to the shapes presented in Figure 9 of the main manuscript, and discussed there in more general terms. As can be seen, the interaction is purely repulsive for all separations considered. However, similar to separations along the x axis, there is again a direct competition between the spring and liquid crystal energies. As can be seen, in Figure S3 I., the inner facing sides in region A are somewhat flattened, in comparison to region B. This reduces the distortion in the region between the particles, but increases the spring energy. The transition from region A to B corresponds to the point where the decrease in spring energy that would occur by having a rounder particle side overcomes the resulting increase in liquid crystal energy. For the particles in Figure S3 II., such a shape change at the larger separations we have considered does not occur, since these particles have a smaller linear spring constant, and therefore would experience a smaller change in spring energy with the shape change which would not be enough to overcome the increase in liquid crystal energy at these separations. This lower spring constant does however allow for additional shape changes at closer separations. As can be seen, in moving from region A to region B, there is a shape change, as the particles become tilted. This change in shape is associated with an increase of $\sim 0.2\ \mu m$ in perimeter length, resulting in an increase in the spring energy; however there is also an increase of $\sim 0.1\ \mu m$ in the total distance between all pairs of the like defects (compared to particles at the same locations, but with the same shapes as those in region A), resulting in a decrease in the liquid crystal energy. Since the linear spring constant is smaller in this case compared to that of Figure S3 I., the decrease in liquid crystal is enough to overcome the increase in spring energy associated with this shape change.

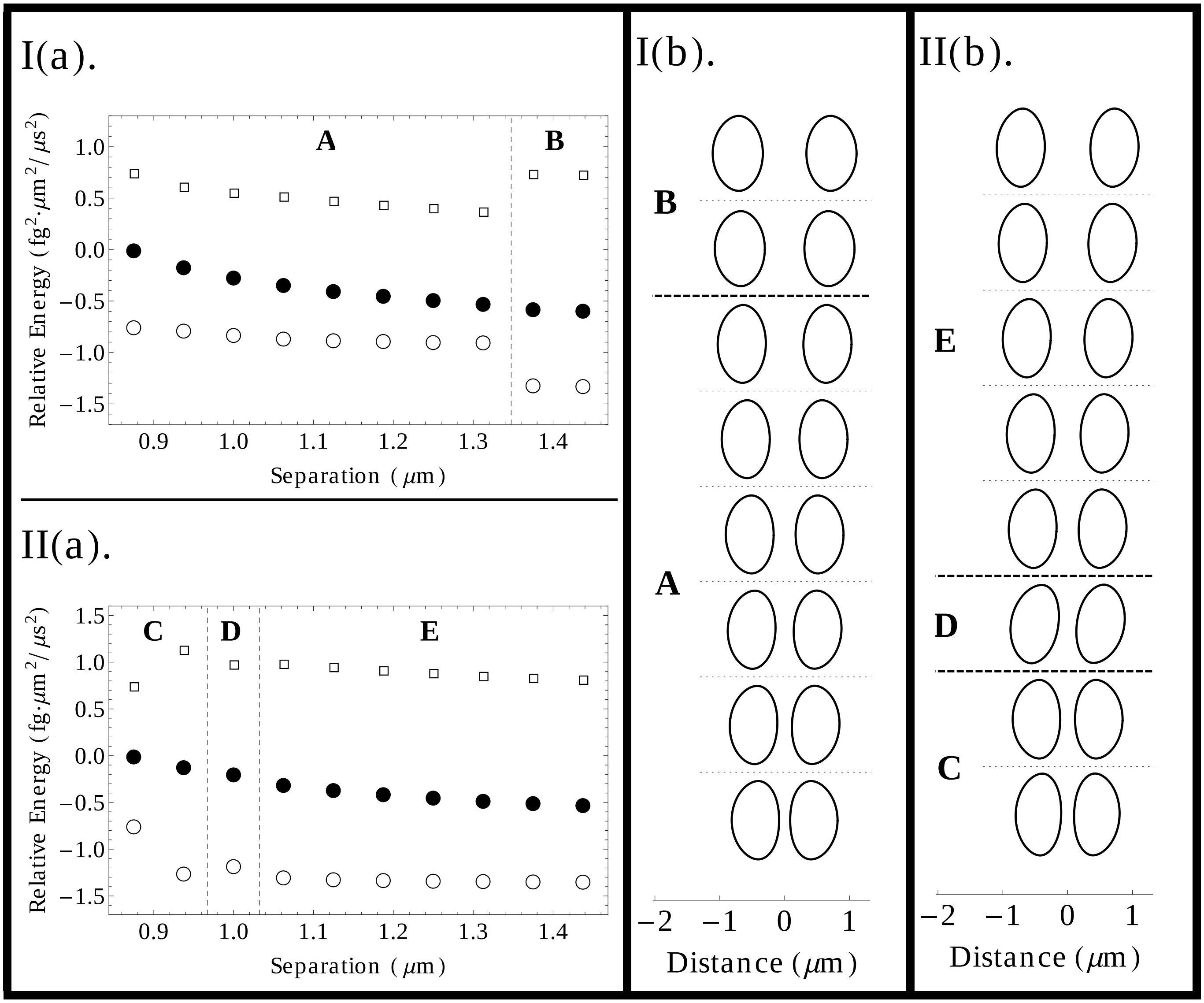

Fig. S3 Interaction between deformable particles separated along the y-axis, with the bulk liquid crystal director orientation along this same axis. Here, hollow circles represent the elastic energy of the springs, which has been shifted so that the closest particle separation corresponds to a value of $-0.75\ fg \cdot \mu m^2/\mu s^2$, hollow squares correspond to the liquid crystal free energy, shifted to $0.75\ fg \cdot \mu m^2/\mu s^2$ for the closest separation, and the total system energy, which is set to $0.0\ fg \cdot \mu m^2/\mu s^2$ at closest separation, is denoted by filled circles. Panel I: spring constants $k_1 = 0.2,\ k_2 = 4.0$. Panel II: $k_1 = 0.1,\ k_2 = 4.0$.